Photoaffinity Cross-Linking of Alzheimer's Disease Amyloid Fibrils Reveals Interstrand Contact Regions between Assembled β-Amyloid Peptide Subunits†

Gregory F. Egnaczyk,‡ Kenneth D. Greis,§ Evelyn R. Stimson,‡ and John E. Maggio*,‡

Department of Pharmacology & Cell Biophysics, University of Cincinnati College of Medicine, 231 Albert Sabin Way, P.O. Box 670575, Cincinnati, Ohio 45267-0575, and Procter & Gamble Pharmaceuticals Health Care Research Center, 8700 Mason-Montgomery Road, P.O. Box 8006, Mason, Ohio 45040

Received December 15, 2000; Revised Manuscript Received June 22, 2001

ABSTRACT: The assembly of the β-amyloid peptide (Aβ) into amyloid fibrils is essential to the pathogenesis of Alzheimer's disease. Detailed structural information about fibrillogenesis has remained elusive due to the highly insoluble, noncrystalline nature of the assembled peptide. X-ray fiber diffraction, infrared spectroscopy, and solid-state NMR studies performed on fibrils composed of Aβ peptides have led to conflicting models of the intermolecular alignment of β-strands. We demonstrate here the use of photoaffinity cross-linking to determine high-resolution structural constraints on Aβ monomers within amyloid fibrils. A photoreactive $A\beta_{1-40}$ ligand was synthesized by substituting L-*p*-benzoylphenylalanine (Bpa) for phenylalanine at position 4 ($A\beta_{1-40}$ F4Bpa). This peptide was incorporated into synthetic amyloid fibrils and irradiated with near-UV light. SDS−PAGE of dissolved fibrils revealed the light-dependent formation of a covalent Aβ dimer. Enzymatic cleavage followed by mass spectrometric analysis demonstrated the presence of a dimer-specific ion at $MH^+ = 1825.9$, the predicted mass of a fragment composed of the N-terminal $A\beta_{1-5}$ F4Bpa tryptic peptide covalently attached to the C-terminal $A\beta_{29-40}$ tryptic peptide. MS/MS experiments and further chemical modifications of the cross-linked dimer led to the localization of the photo-cross-link between the ketone of the Bpa4 side chain and the δ-methyl group of the Met35 side chain. The Bpa4−Met35 intermolecular cross-link is consistent with an antiparallel alignment of Aβ peptides within amyloid fibrils.

The amyloidoses are a group of more than 20 human diseases that have as their common feature the assembly of a naturally occurring soluble protein or peptide into insoluble deposits with distinct tinctorial properties and fibrillar morphology (*1*). The offending proteins vary widely in molecular weight, amino acid composition, and sequence but share the ability to assemble into well-ordered, β-pleated sheet fibrils termed amyloids.

Alzheimer's disease (AD)[1] is the most common amyloidosis of the brain and the leading cause of dementia, affecting over 4 million elderly individuals in the United States alone (*2*). The pathognomonic lesion of AD, the amyloid plaque, was first described in 1906 by Alois Alzheimer (*3*). The amyloid plaques consist mainly of the ∼40 residue β-amyloid peptide (Aβ). The self-assembly of the Aβ peptide into fibrils is seminal to the pathogenesis of Alzheimer's disease, as demonstrated by several lines of evidence (*4*−*10*). In particular, it appears that an oligomeric form of Aβ is required for in vitro and in vivo neurotoxicity (*11*−*15*). The conditions under which these Aβ aggregates form in vivo and how they mediate neurotoxicity are not well understood. Elucidation of the molecular structure of the fibrils should assist in the explanation of these pathogenic processes and aid in design of agents to inhibit assembly.

The development of a high-resolution molecular structure of amyloid fibrils has been hindered by their insoluble, noncrystalline nature. Several different methods have been employed to elucidate the structure of amyloid fibrils, including X-ray fiber diffraction, Fourier transform infrared spectroscopy (FTIR), and solid-state NMR (SSNMR). X-ray diffraction patterns from Aβ amyloid fibrils demonstrate two principal reflections. A meridional reflection at 4.8 Å and an equatorial reflection at 10 Å characterize the interstrand and intersheet distances, respectively, within the amyloid structure (*16*). The data are consistent with a cross-β structure in which the β-sheets and the extended polypeptide backbones are perpendicular to the long axis of the fibril (*17*). FTIR data confirm the β-sheet structure of amyloid fibrils and go further to suggest an antiparallel alignment of β-strands (*18*, *19*). This model is based upon the observation of amide I absorption bands at roughly 1690 and 1630 cm^{-1}, bands characteristic of antiparallel β-sheets in model peptides (*20*).

† This work was supported by the National Institutes of Health Grant AG12853.

* To whom correspondence should be addressed. Phone: (513) 558-2354. Fax: (513) 558-1169. E-mail: John.Maggio@uc.edu.

‡ University of Cincinnati College of Medicine.

§ Procter & Gamble Pharmaceuticals Health Care Research Center.

[1] Abbreviations: Aβ, β-amyloid peptide; AD, Alzheimer's disease; Bpa, L-*p*-benzoylphenylalanine; CHCA, α-cyano-4-hydroxycinnamic acid; DRAWS, dipolar coupling in a windowless sequence; EM, electron microscopy; ESI-IT MS, electrospray ionization−ion trap mass spectrometry; FTIR, Fourier transform infrared spectroscopy; HFIP, hexafluoro-2-propanol; HPLC, high-performance liquid chromatography; MALDI-TOF MS, matrix-assisted laser desorption ionization−time of flight mass spectrometry; MH^+, monoisotopic mass plus mass of a proton; MS/MS, tandem mass spectrometry; *m*/*z*, mass/charge; Nle, norleucine; SSNMR, solid-state nuclear magnetic resonance spectroscopy; TFA, trifluoroacetic acid.

10.1021/bi002852h CCC: $20.00
Published on Web 09/07/2001

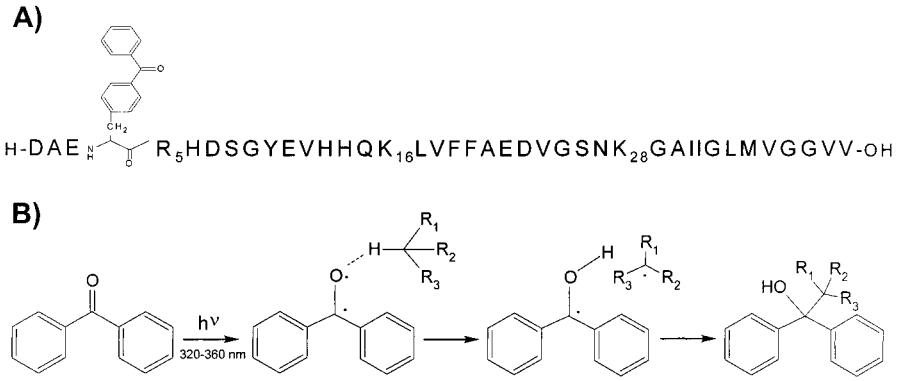

FIGURE 1: Photoreactive Aβ_{1-40} F4Bpa. (A) Aβ_{1-40} F4Bpa. The three basic amino acids are noted with position number. (B) Reaction scheme illustrating the photoactivation and photoinsertion of the benzophenone moiety of Bpa.

A technique that has the potential to produce high-resolution molecular structural models of amyloid fibrils is solid-state NMR. Fibrils formed from four different Aβ peptides have been analyzed by SSNMR. Lansbury, Griffin, and co-workers characterized fibrils made from the C-terminal fragment Aβ_{34-42} (*21*). They determined that the alignment of Aβ_{34-42} fibrils is antiparallel and two residues out of register using rotational resonance experiments on doubly ^{13}C-labeled samples. Lynn, Meredith, Botto, and co-workers studied amyloid fibrils composed of Aβ_{10-35} (*22*−*24*), a fragment that contains the hydrophobic core region (Leu17-Ala21) of Aβ, a region essential for both the aggregation and deposition of Aβ (*25*, *26*). They implemented the DRAWS pulse sequence to measure distances between ^{13}C nuclei within fibrils composed of peptides containing a single label in one amino acid. Their data are consistent with a parallel alignment of molecules in direct register. More recently, Tycko and colleagues have performed multiple-quantum SSNMR experiments to assess the proximity of spin labels within fibrils composed of the full-length Aβ_{1-40} molecule (*27*). As in the case of Aβ_{10-35}, their data best matches simulated data generated from a parallel alignment model with Aβ molecules in direct register. Tycko and colleagues also analyzed fibrils composed of the central hydrophobic fragment Aβ_{16-22}, end capped with acetyl and amide groups at the N- and C-termini (*28*). SSNMR data are consistent with an antiparallel alignment for this peptide. In sum, SSNMR studies have presented evidence for both parallel and antiparallel alignments of Aβ fragments, depending on the peptide sequence studied and the methodology employed.

To characterize the relative orientation of Aβ molecules within amyloid fibrils, we employed photoaffinity cross-linking to identify points of proximity between adjacent Aβ molecules. The photoreactive amino acid L-*p*-benzoylphenylalanine (Bpa) has proven extremely useful in identifying sites of interaction between a photolabile peptide ligand and its receptor (*29*−*32*). Photoaffinity labeling with Bpa is highly efficient and generally results in modification of a single site (*33*, *34*). Photoactivated (triplet biradical) Bpa is essentially inert toward water, reacting preferentially by insertion into C−H bonds of any amino acid (Figure 1B), although it may prefer photoinsertion into amino acids containing heteroatoms (*35*). Other advantages of Bpa include chemical stability and activation at near-UV wavelengths (>320 nm), wavelengths greater than those that typically damage proteins. In this study Bpa was incorporated into a full-length Aβ_{1-40} molecule and used as a probe to determine specific interactions between amino acids on adjacent β-strands within the fibrillar structural context. Aβ_{1-40} F4Bpa was diluted with wild-type Aβ_{1-40} peptide, assembled into synthetic fibrils, and covalently photo-cross-linked. Fibrils were dissolved, and the position of the photoinsertion within the cross-linked dimers was determined by a series of enzymatic and chemical modifications analyzed by mass spectrometry. This analysis established an intermolecular cross-link between Bpa4 and Met35. This work presents direct biochemical evidence for the antiparallel arrangement of subunits within amyloid fibrils of full-length Aβ.

EXPERIMENTAL PROCEDURES

Synthetic Peptides. Synthetic Aβ_{1-40}-OH and Aβ_{1-40}-OH F4Bpa (purity >95%) were purchased from Quality Controlled Biochemicals (Hopkinton, MA), and Aβ_{1-40}-NH$_2$ M35Nle was a gift from Dr. Jonathan Lee (Boston University). Peptides were characterized by reverse-phase HPLC, MALDI-TOF mass spectrometry, and amino acid analysis and gave satisfactory results in all cases.

Radioiodination. Aβ_{1-40} and Aβ_{1-40} F4Bpa peptides were radioiodinated as previously described (*36*). Briefly, the peptides were radiolabeled by oxidative iodination using Na^{125}I and chloramine-T. The radiolabeled Aβ was reduced in 20% 2-mercaptoethanol at 90 °C for 90 min and then purified by reverse-phase HPLC to essentially quantitative specific activity (approximately 2000 Ci/mmol). Several studies have established that ^{125}I-Aβ behaves indistinguishably from native Aβ in a variety of experiments (*37*−*39*).

Preparation of Bpa-Containing Aβ Fibrils. Fibrillar Aβ aggregates were prepared from solutions of 10^{-4} M Aβ in PBS (10 mM sodium phosphate, 100 mM NaCl, pH 7.4). To produce radiolabeled, Bpa-containing Aβ fibrils, ^{125}I-labeled Aβ_{1-40} F4Bpa peptide was added to unlabeled peptide in PBS to yield a molar ratio of F4Bpa to wild-type Aβ of 1:10^5. For cold Bpa-containing Aβ fibrils, the molar ratio of F4Bpa to wild-type (or M35Nle) Aβ was approximately 1:10. Immediately following dissolution, peptide solutions were vigorously agitated (Teflon-coated stir bar at 800 rpm) at room temperature for 20−24 h (*40*). This protocol typically results in aggregation of >80% of the starting peptide into fibrillar, insoluble, congophilic material sedimentable at 14000*g*. Reverse-phase HPLC of the tryptic peptides from dissolved cold Bpa4-containing fibrils confirmed that the

ratio of F4Bpa:wild-type Aβ in the fibrils was approximately 10%.

Electron Microscopy. EM grids were prepared essentially as described previously (*17*). Briefly, 10 μL of suspended Aβ fibrils prepared as described above was applied to carbon-coated Formvar grids (Electron Microscopy Sciences, Washington, PA) and incubated for 2 min. The droplet was then displaced with an equal volume of 0.5% (v/v) glutaraldehyde solution and incubated for an additional 60 s. The grid was then washed with water. Ten microliters of 2% (w/v) uranyl acetate solution was applied to the grid and incubated for 2 min. The grid was gently blotted with filter paper and subsequently air-dried. Samples were examined using a JEOL CX100 electron microscope.

Photoaffinity Labeling of Aβ Fibrils. Aβ fibrils were sedimented by centrifugation (10 min at 14000*g*). The pellet was resuspended and centrifuged again to remove any unaggregated peptide. The pellet was resuspended in PBS and vortexed vigorously to produce a fine particulate suspension. The suspension was then transferred onto a polypropylene platform as a large droplet. The platform was placed into a Rayonet photochemical reactor (Southern New England Ultraviolet Co., Hamden, CT) equipped with 3500 Å lamps. The fibrils were irradiated for 2 h on ice and recovered from the platform, pelleted, and washed.

SDS−PAGE Analysis of Dissociated Fibrils. Aβ fibrils were dissolved in 88% formic acid, diluted 10-fold with double distilled water, frozen, and lyophilized. The lyophilizates were dissolved in hexafluoro-2-propanol (HFIP), concentrated under N_2, and then mixed with SDS sample buffer. Tris−Tricine SDS−PAGE was performed as described by von Jagow et al. (*41*). Autoradiography or Coomassie Blue staining was used for detection of peptide bands. Cold (not radiolabeled) peptides were employed for all proteolysis and mass spectrometry experiments.

In-Gel Trypsin Digest. In-gel digestion was performed essentially as described by Shevchenko et al. (*42*). Briefly, cold Aβ monomer and dimer gel bands were separately excised and destained with 25 mM ammonium bicarbonate in 50% acetonitrile. Gel bands were cut into 1 mm^3 cubes and dried in a vacuum centrifuge for 20 min. The dried gel pieces were rehydrated with 0.10 mg/mL sequence-grade trypsin (Promega, Madison, WI) in 25 mM ammonium bicarbonate (pH 8). After rehydration the gel was overlaid with 25 mM ammonium bicarbonate and incubated at 37 °C for 16−20 h. The digest solution was removed and saved. Tryptic peptides were then extracted from the gel pieces with 20 μL of 50% acetonitrile/5% trifluoroacetic acid (TFA) solution; this step was repeated twice. The extracts were pooled with the digest solution and concentrated to <10 μL in a vacuum centrifuge. The peptide solution was then diluted to 25 μL with 0.3% TFA and prepared for MALDI-TOF MS.

Matrix-Assisted Laser Desorption Ionization−Time of Flight Mass Spectrometry (MALDI-TOF MS). Aβ tryptic peptide extracts were concentrated and desalted by reverse-phase adsorption (C18 ZipTips, Millipore, Framingham, MA). The tryptic peptides were eluted from the solid phase directly onto the MALDI sample plate with a 50% acetonitrile/0.3% TFA solution containing the matrix, α-cyano-4-hydroxycinnamic acid (CHCA), at 10 mg/mL. MALDI-TOF mass spectrometry was performed using a Perseptive Biosystems Voyager DE Pro (Framingham, MA). Spectra were internally calibrated using autoproteolytic fragments of trypsin. Theoretical masses (MH^+) for tryptic peptides were calculated using the MS-Digest module of Protein Prospector (http://prospector.ucsf.edu/, 2000). Spectra were processed in the software program m/z (Proteometrics Canada Ltd.).

Electrospray Ionization−Ion Trap Mass Spectrometry (ESI-IT MS). Cold cross-linked fibrils were dissolved in 88% formic acid. The solution was diluted 10-fold with doubly distilled water, frozen, and lyophilized. The lyophilizate was dissolved in 25 mM ammonium bicarbonate, and sequence-grade trypsin was added at a 1:20 weight ratio of trypsin to Aβ peptide. The solution was incubated at 37 °C for 16−20 h. One volume of 0.3% TFA was added to quench the reaction, and the solution was concentrated to <10 μL. Samples were then diluted with 50% acetonitrile/0.1% TFA and infused directly into the mass spectrometer at 4 μL/min. Mass spectra were collected by ESI-IT mass spectrometry using a ThermoQuest/Finnigan LCQ^{Deca} (San Jose, CA). MS/MS data were obtained by isolation of $MH^+ = 1825.9$ in the ion trap followed by fragmentation at 35 V and mass analysis of the resulting product ions. Ion time was set below 10 ms to minimize the space-charging effects due to ions of the more abundant, non-cross-linked tryptic peptides. Theoretical masses for product ions from both $A\beta_{1-5}$ F4Bpa and $A\beta_{29-40}$ tryptic fragments were calculated using the MS-Product module of Protein Prospector (http://prospector.ucsf.edu/, 2000).

Methylation/Elimination of Methionine 35. Cold Aβ fibrils were dissolved in 88% formic acid solution, diluted 10-fold with water, frozen, and lyophilized. The lyophilizates were dissolved in a 2 M urea/150 mM potassium dihydrogen phosphate (KH_2PO_4) solution titrated to pH 3 with HCl; neat methyl iodide was added to 5% (v/v). The solution was incubated at room temperature for 18−24 h in the dark. The peptides were digested with trypsin and processed for MALDI-TOF mass spectroscopy as described above.

Dehydration of Cross-Linked Dimers. Cold Aβ fibrils were dissolved in 88% formic acid solution and incubated at room temperature for 18 h. Dehydrated samples were diluted 10-fold, frozen, and lyophilized. For dehydration/methylation experiments, dehydrated sample lyophilizates were dissolved in 2 M urea and 150 mM potassium phosphate (pH 3), incubated with neat methyl iodide, digested with trypsin, and processed for MALDI-TOF mass spectroscopy as described above.

RESULTS

Electron Microscopy of $A\beta_{1-40}$ F4Bpa Fibrils. $A\beta_{1-40}$ peptide fibrils containing a trace amount of the photoreactive peptide $A\beta_{1-40}$ F4Bpa (Figure 1A) were examined by transmission EM to assess their ultrastructure. Representative electron micrographs are shown in Figure 2. The fibrillar morphology is indistinguishable from that of synthetic fibrils made entirely of $A\beta_{1-40}$ and compares well with the morphology of ex vivo fibrils from the plaques of AD patients (*17*). The average diameter of the fibrils was 7.5 nm, and most fibrils were greater than 100 nm in length. Other observed properties characteristic of amyloid fibrils include their unbranching nature and an apparent periodic twist (Figure 2B).

Table 1: Cross-Linked Tryptic Fragments[a]

	DAEFR (637.3 Da)	HDSGYEVHHQK (1336.6 Da)	LVFFAEDVGSNK (1325.7 Da)	GAIIGLMVGGVV (1085.6 Da)
+DAE[Bpa]R (741.3 Da) theoretical cross-linked fragment	1377.6	2076.9	2066.0	1825.9
observed peak	none	none	none	1825.9

[a] Molecular masses given are MH^+ values.

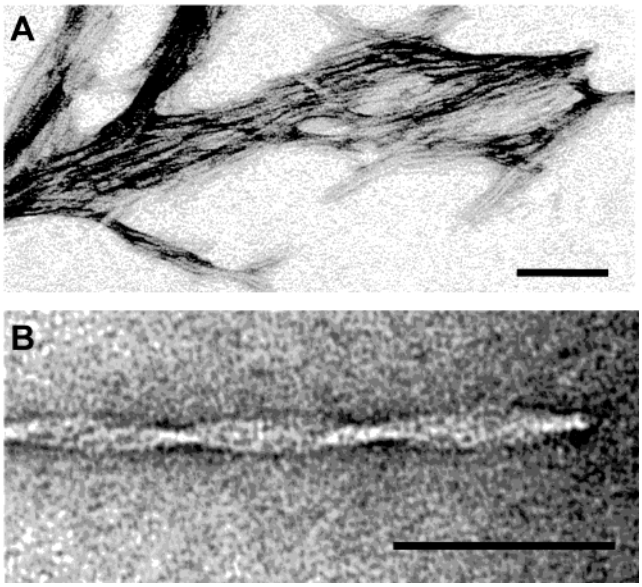

FIGURE 2: Morphology of amyloid fibrils containing Aβ_{1-40} F4Bpa. Fibrils were prepared from a mixture of Aβ_{1-40} and Aβ_{1-40} F4Bpa peptides and examined by transmission EM. (A) Negatively stained fibrils. (B) A single amyloid fiber. Scale bars are 100 nm.

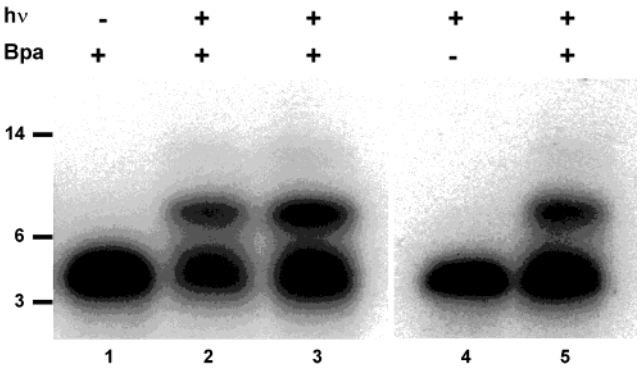

FIGURE 3: Aβ_{1-40} F4Bpa forms cross-linked dimers upon irradiation with near-UV light. Aβ_{1-40} fibrils containing ^{125}I tracer were photolyzed, dissolved in formic acid, lyophilized, dissolved in HFIP, and electrophoresed on Tris−Tricine gels followed by autoradiography. Bpa-containing fibrils in the absence (lane 1) and the presence (lanes 2, 3, and 5) of near-UV light. Wild-type Aβ_{1-40} fibrils in the presence of near-UV light (lane 4).

SDS−PAGE Separation of Monomers and Cross-Linked Dimers. Aβ_{1-40} fibrils containing a trace amount of ^{125}I Aβ_{1-40} F4Bpa were utilized to assess the ability of the photoreactive molecule to covalently cross-link Aβ molecules within amyloid fibrils. Tris−Tricine SDS−PAGE was implemented to separate monomers from cross-linked dimers (Figure 3). Following irradiation with near-UV light, a band was detected at 8−9 kDa, the expected size of an Aβ dimer. This dimer band was dependent upon both photoirradiation and the presence of the photophore, a result that argues strongly that an *inter*molecular covalent cross-link has formed.

In-Gel Trypsin Digest Reveals a Cross-Linked Fragment. To determine the position of the photoinsertion, both the monomer and dimer bands from nonradioactive samples were excised and digested with trypsin. The tryptic peptides were extracted and analyzed by MALDI-TOF mass spectrometry. The reaction scheme of the photoinsertion (Figure 1B) reveals that there is no net gain or loss of mass upon recombination. Table 1 shows the four tryptic peptides (Aβ_{1-5}, Aβ_{6-16}, Aβ_{17-28}, and Aβ_{29-40}) produced in a complete digest of Aβ_{1-40}, the potential cross-linked fragments that could result, and their predicted MH^+. The mass spectra of the tryptic digests from both the monomer and dimer bands are shown in Figure 4. Inspection of the mass spectra reveals the presence of an ion at *m*/*z* 1825.9 in the dimer band digest but not in the monomer band digest (Figure 4, inset). No other potential cross-linked fragments were detected. This cross-linked fragment indicates that Bpa4 inserted into the C-terminal tryptic fragment Aβ_{29-40}. The presence of a +16 Da peak (1841.9) indicates the partial oxidation of Met35 to sulfoxide, further supporting the conclusion that the Aβ_{29-40} peptide makes up part of the cross-linked fragment.

Ion Trap Mass Spectrometry. To obtain more detailed structural information on the cross-linked fragment, MS/MS spectra were acquired utilizing ESI-IT mass spectrometry. Tryptic digests of photoirradiated fibrils were directly infused into the instrument. The cross-linked tryptic fragment was detected at $MH^+ = 1825.9$. Multiply charged species of the cross-linked peptide were not detected; therefore, the singly charged ion, $MH^+ = 1825.9$, was isolated in the trap and subsequently fragmented (Figure 5). The assignment of fragment ions produced in the MS/MS experiment is given in Table 2. Cleavage events on the Aβ_{1-5} F4Bpa peptide segment of the cross-linked 1825.9 ion produce y series (C-terminal) ions whereas cleavage of the Aβ_{29-40} peptide produces b series (N-terminal) ions. This cleavage pattern is consistent with the fragment ion series observed in MS/MS spectra of the un-cross-linked peptides (data not shown). Two fragment ions from the 1825.9 precursor ion contain the b_7 ion (NH_3^+-GAIIGLM) from the Aβ_{29-40} peptide. The MS/MS data provide additional support for the conclusion that the light-dependent 1825.9 ion seen in the MALDI-TOF mass spectra is composed of the N-terminal Aβ_{1-5} F4Bpa peptide cross-linked into the C-terminal Aβ_{29-40} peptide. Furthermore, these data establish that Bpa4 cross-linked into one of seven amino acids (GAIIGLM) within the 12-mer C-terminal peptide.

Further attempts to define the exact position of the cross-link by additional fragmentation of the product ions of 1825.9 were unsuccessful due to the relatively low abundance of the precursor ion at 1825.9 compared to the non-cross-linked

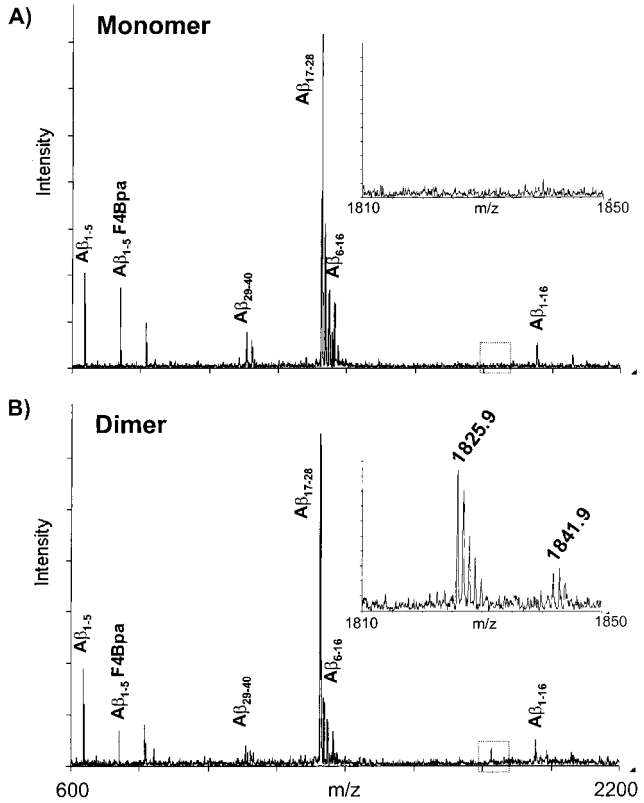

FIGURE 4: MALDI-TOF mass spectra demonstrate the presence of a light-dependent cross-linked fragment. Monomer and dimer bands were excised from the gel and digested with trypsin. The peptides were extracted and analyzed by MALDI-TOF MS. (A) Mass spectrum of peptides from the monomer band digest. (B) Mass spectrum of peptides from the dimer band digest. The inset in each panel displays a region of the respective spectrum expanded to show the $MH^+ = 1825.9$ ion, present only in the cross-linked dimer. The peak at 1825.9 Da represents the cross-linked fragment containing the N-terminal Aβ_{1-5} F4Bpa and the C-terminal Aβ_{29-40} peptides. The peak at 1841.9 Da represents the sulfoxide (+16 Da) of that cross-linked fragment.

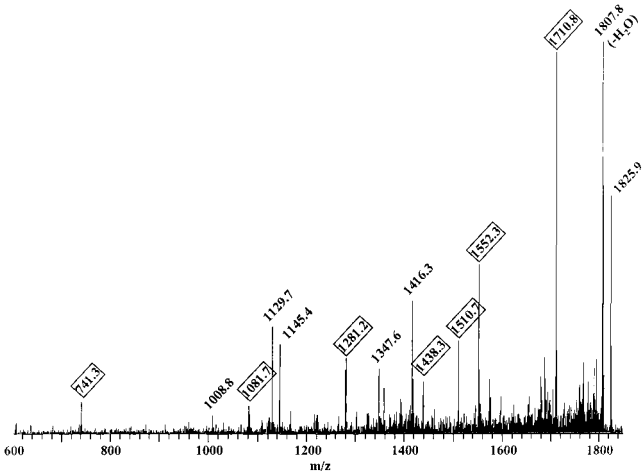

FIGURE 5: MS/MS fragmentation of the cross-linked tryptic peptide. The cross-linked peptide at $MH^+ = 1825.9$ was isolated in the ion trap and fragmented as described in Experimental Procedures. A detailed summary of the assigned fragment ions (masses highlighted with boxes) is provided in Table 2.

tryptic peptides. Thus space-charging effects limited the total number of ions that could be resolved in the trap. Space-charging occurs when too many ions are captured in an ion trap at a given time, resulting in altered resolution and

Table 2: Fragment Ions from MS/MS of 1825.9

fragment ion[a]	Aβ_{1-5} F4Bpa ion[b]	Aβ_{29-40} ion[c]	structure
1710.6	y_4	full	AE*Bpa*R GAIIGLMVGGVV
1552.3	full	b_9	DAE*Bpa*R GAIIGLMVG
1510. 7	y_2	full	*Bpa*R GAIIGLMVGGVV
1438.3	y_4	b_9	AE*Bpa*R GAIIGLMVG
1281.2	y_4	b_7	AE*Bpa*R GAIIGLM
1081.6	y_2	b_7	*Bpa*R GAIIGLM
741.3	full	none	DAE*Bpa*R

[a] Values provided for fragment ions are in daltons. The ions are singly charged (MH^+). [b] y series ions are fragment ions that retain the C-terminus. [c] b series ions are fragment ions that retain the N-terminus.

inaccurate mass measurements (*43*). The net effect is that lower abundance ions (such as $MH^+ = 1825.9$ in this experiment) can broaden to the point in which they are indistinguishable from background. To circumvent space-charging, it was necessary to shorten the ion time (the time in which ions are allowed to enter the ion trap) to less than 10 ms. This approach, however, also limited our ability to generate sequential fragments to completely map the site of cross-linking. Therefore, other means of determining the position of the cross-link were examined. Attempts to isolate the cross-linked peptide from the more abundant tryptic peptides by HPLC with multiple types of columns and elution conditions were unsuccessful. Instead, chemical modification approaches were employed to refine the cross-link position.

Methylation of Methionine 35. Examination of the amino acid composition of Aβ_{29-40} reveals only one likely position for protonation (charging)—at the N-terminus. Addition of more charge to that peptide should increase the number of fragment ions produced in MS/MS experiments. To achieve the placement of more charge on the Aβ_{29-40} peptide, we methylated the sulfur atom of Met35 to produce the methylsulfonium cation. MALDI-TOF MS analysis of the tryptic digest of methylated peptides did not reveal an ion at $MH^+ = 1099.6$, corresponding to methylation of methionine (+14 Da), nor was the unmodified peptide observed (1085.6 Da). Instead, we repeatedly observed an ion at $MH^+ = 1037.6$, a mass difference of −48 Da. This same mass loss (−48 Da) has been reported upon alkylation of methionine side chains in peptides (*44*). After formation of the sulfonium ion ($\Delta m = +14$), a β-elimination reaction follows, with the dimethyl thioether as the leaving group ($\Delta m = -62$), giving a net loss of 48 Da (Figure 6A). Taking advantage of this sulfur-specific chemistry, we tested the hypothesis that Bpa4 cross-linked into Met35. Figure 6B demonstrates the reaction scheme utilized to test the hypothesis and the monoisotopic mass of the expected products. MALDI-TOF mass spectra demonstrate the presence of the intermediate and end products of the proposed chemistry. In particular, an ion at $MH^+ = 803.3$ was detected in the photolyzed fibril digest (Figure 6D) but not in the control digest (Figure 6C). The presence of the light-dependent $MH^+ = 803.3$ ion is consistent with the hypothesis that Bpa photophore has photoinserted into the distal methyl group of the methionine side chain. A smaller peak at $MH^+ = 1777.9$ ($\Delta m = -48$)

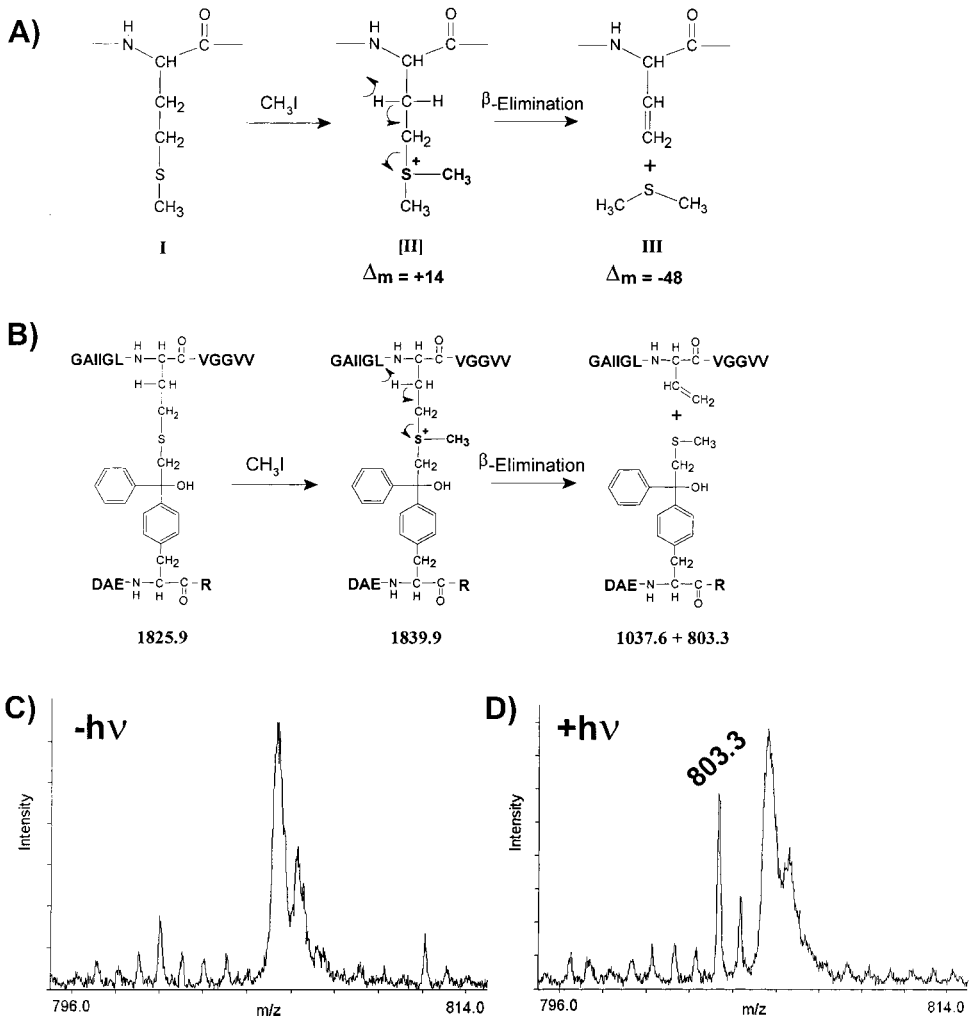

FIGURE 6: Methylation/elimination of cross-linked Aβ dimers. Formic acid dissolved fibrils were methylated with methyl iodide. The peptides were digested with trypsin and analyzed by MALDI-TOF MS. (A) Reaction scheme illustrating methylation of methionine which leads to the specific cleavage of its side chain. (B) Reaction scheme illustrating the products and their MH^+ values resulting from the methylation of the cross-linked fragment. (C) Mass spectrum of the control ($-h\nu$) sample. (D) Mass spectrum of the photolyzed ($+h\nu$) sample demonstrating the presence of an ion at $MH^+ = 803.3$.

was detected in the photolyzed fibril digest as well, consistent with insertion into the γ-methylene group of the methionine side chain; however, this peak does not unambiguously assign the position of the photoinsertion to methionine.

Acid-Catalyzed Dehydration of the Cross-Linked Dimer. Incubation of irradiated fibrils in 88% formic acid for extended periods of time (>16 h) results in the dehydration loss of the hydroxyl group formed during photo-cross-linking (Figure 7A). Mass spectrometry demonstrates the loss of the 1825.9 ion intensity and the appearance of an 1807.9 ion (Figure 7B), indicating the loss of a water molecule ($\Delta m = -18$ Da). This chemistry appears to be specific for the hydroxyl group of the covalent cross-link bond, whose loss produces a conjugated π-system (Figure 7A). Dehydrated cross-linked dimers were methylated and digested with trypsin and the products analyzed by MALDI-TOF MS. The expected products are the dehydrated (−18 Da) forms of the species shown in Figure 6B. The mass spectra indicate the presence of an ion at $MH^+ = 785.3$ that is light-dependent (Figure 7C,D). These data further strengthen the conclusion that the ketone group of the Bpa4 side chain photoinserts into the δ-methyl group of the Met35 side chain (Figures 6B and 7A), indicating their close proximity within amyloid fibrils composed of Aβ_{1-40}.

Photoinsertion of Bpa4 into the C-Terminal Peptide Aβ_{29-40}-NH_2 M35Nle. Photoactivated Bpa may prefer insertion into amino acids that contain heteroatoms, such as methionine with its electrophilic sulfur atom. To address this potential preference, we prepared amyloid fibrils composed of an Aβ peptide in which norleucine replaces methionine at position 35 (Aβ_{1-40}-NH_2 M35Nle). This fibril preparation also contains the unradiolabeled Bpa4 molecule to allow for photoaffinity cross-linking. The mass difference between norleucine and methionine is −18 Da, the same mass difference produced by dehydration. To avoid potential ambiguity between the cross-linked fragment containing the M35Nle peptide and the dehydrated form of the cross-linked fragment containing Met35 (1807.9) as described in Figure 7, we used a carboxamidated Aβ_{1-40} M35Nle peptide. The amidation changes the molecular weight of the C-terminal peptide by −1 Da. Therefore, the overall Δm between the wild-type, free acid peptide and the M35Nle amide peptide is −19 Da. The predicted MH^+ of a cross-linked fragment containing the N-terminal tryptic peptide Aβ_{1-5} F4Bpa and

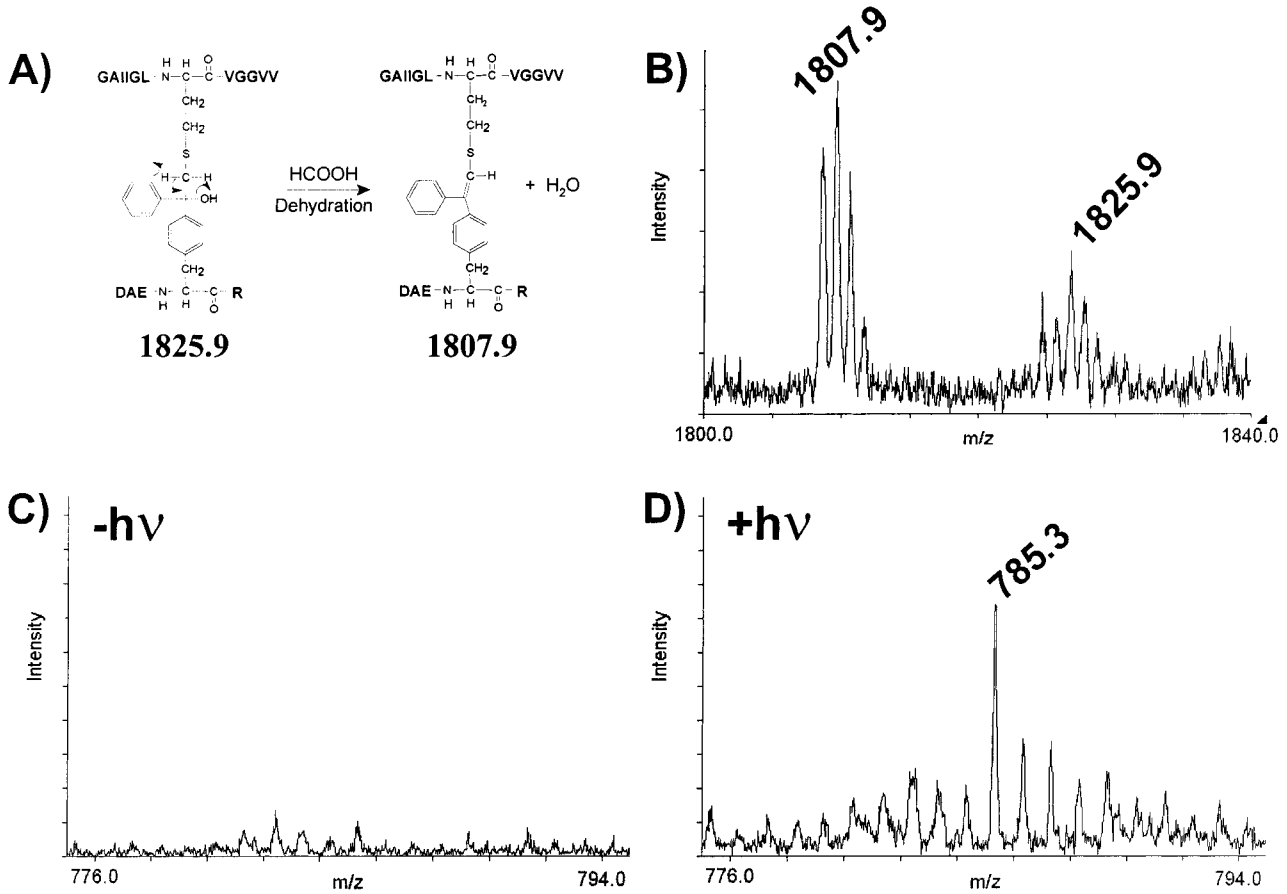

FIGURE 7: Dehydration of cross-linked Aβ dimers. Fibrils ($\pm h\nu$) were incubated in formic acid for 18 h and then methylated for an additional 24 h. The peptides were digested with trypsin and analyzed by MALDI-TOF MS. (A) Reaction scheme illustrating the acid-catalyzed dehydration of the cross-linked fragment. (B) Mass spectrum demonstrating the dehydrated cross-linked fragment $MH^+ = 1807.9$. (C) Mass spectrum of the control ($-h\nu$) sample. (D) Mass spectrum of the photolyzed ($+h\nu$) sample demonstrating the presence of an ion at $MH^+ = 785.3$.

the C-terminal tryptic peptide Aβ_{29-40} M35Nle equals 1806.9 Da. This peak and its dehydrated form (1788.9) were observed in photoirradiated fibrils and not detected in fibrils that were not exposed to near-UV light. This result demonstrates that methionine need not be present in order for Bpa4 to insert into the C-terminal region of an adjacent Aβ peptide. Furthermore, this result establishes that an *inter*molecular cross-link is formed, since an intramolecular photoinsertion would produce a cross-linked fragment containing Met35 in the C-terminal tryptic peptide.

DISCUSSION

Despite an extensive body of literature on the structure of Aβ amyloid fibrils, the question of whether the β-strands are arranged in parallel or antiparallel remains unresolved. Amyloid fibrils are noncrystalline in nature, and the diffraction patterns from the fibers can only be interpreted with limited resolution. Diffraction data from fibrils formed from various fragments of Aβ have detected faint meridional reflections at 9.4 Å (*17*, *45*). This reflection, demonstrating a pattern spacing of two interstrand intervals, is strongly suggestive of an antiparallel alignment of β-strands. IR studies performed on Aβ in the solid state are also consistent with an antiparallel alignment (*18*, *19*). Solid-state NMR experiments have provided the highest resolution structural data on amyloid fibrils to date. The fibrillar structure of four different Aβ peptides have been analyzed using very different experimental designs to probe the intramolecular and intermolecular $^{13}C-^{13}C$ distances within synthetic fibrils composed of spin-labeled Aβ peptides. Lansbury, Griffin, and co-workers concluded from SSNMR experiments of Aβ_{34-42} fibrils that the peptide subunits existed in an extended conformation with antiparallel alignment two amino acids out of register (*21*). Lynn, Meredith, Botto, and co-workers interpreted their data on Aβ_{10-35} fibrils as consistent with a model of β-strands in parallel alignment and in direct register (*22*). Tycko and colleagues studied fibrils composed of the full-length Aβ_{1-40} peptide (*27*) and an Aβ fragment containing the hydrophobic core (Aβ_{16-22}) (*28*). Their analysis of the SSNMR data resulted in different models for the alignment of β-strands, one parallel and the other antiparallel. They conclude that the alignment depends on the Aβ congener studied. This conclusion does not concur with the assumption that a specific, organized structure is shared by all amyloids.

The present study demonstrates the application of a novel approach to the elucidation of the intermolecular arrangement of Aβ molecules within the β-sheet ultrastructure of amyloid fibrils. Benzoylphenylalanine has been incorporated into the sequence of the full-length Aβ_{1-40}, replacing phenylalanine at position 4. This molecule (Aβ_{1-40} F4Bpa) was used in photoaffinity cross-linking experiments of amyloid fibrils.

As a minor component of Aβ fibrils, the $A\beta_{1-40}$ F4Bpa molecule does not perturb the ultrastructure of the fibrils as assessed by electron microscopy (Figure 2).

Following photoactivation of the benzophenone group to a triplet biradical, a covalently cross-linked Aβ dimer is formed (Figure 3). Mass spectrometric analysis reveals the presence of a cross-linked fragment (Figure 4) in the tryptic digest of the dimer band and not in the digest of the monomer band. These data taken together with the cross-linked fragments identified from digests of photolyzed amyloid fibrils composed of the M35Nle Aβ peptide argue persuasively that an intermolecular covalent bond has been formed. Considering the small (<3 Å) photoreactive distance range of Bpa (*33*), the cross-link has most likely formed between the side chains of amino acids on neighboring Aβ molecules within the same β-sheet.

A single, dimer-specific MALDI-TOF MS ion was detected at $MH^+ = 1825.9$. This measurement was consistently within 0.10 Da (0.005%) of the MH^+ predicted for a cross-link between the N-terminal and C-terminal tryptic fragments of $A\beta_{1-40}$ (Table 1). MS/MS experiments further corroborated the sequence composition of the cross-linked fragment (Figure 5) and further narrowed the region in which Bpa4 cross-links into the C-terminal peptide to seven amino acids (Gly29−Met35). Due to the technical limitations of space-charge and the inability to recover the peptide by LC-MS, there were insufficient sequence fragment ions to define the exact position of the photoinsertion by sequential MS/MS fragmentation alone.

Chemical modifications specific to the C-terminal peptide $A\beta_{29-40}$ were needed to probe for the exact position of the cross-link. Initially, we attempted methylation of Met35 to produce the sulfonium cation to place more charge on the $A\beta_{29-40}$ peptide to increase the number of fragment (sequencing) ions produced in MS/MS experiments. However, the sulfonium ion was not stable, and its favorable β-elimination resulted in the cleavage of the methionine side chain (Figure 6A). We took advantage of this sulfur-specific chemistry to test the hypothesis that Bpa4 cross-linked into Met35 and to determine the position of the cross-link within the side chains. If the cross-link forms with the terminal methyl group of the methionine side chain, then upon its decomposition the $A\beta_{1-5}$ F4Bpa peptide would contain the leaving group and be 62 Da heavier. Consistent with the hypothesis, a light-dependent peak was observed at 803.3 Da. We also detected a smaller peak at $MH^+ = 1777.9$ that is consistent with insertion into the γ-methylene group of the methionine side chain; however, this result could also be explained by insertion into other amino acids of the $A\beta_{29-40}$ peptide. In contrast, the 803.3 peak is decisive in its assignment of the photoinsertion location to the δ-methyl group of the methionine side chain. To confirm that the 803.3 ion was indeed the ion proposed, we performed the same chemistry on dehydrated cross-linked fibrils. This would result in products that were 18 Da lighter than those proposed in Figure 6B. Consistent with the hypothesis, a light-dependent peak was observed at 785.3 Da. Taken together, the data from Figures 6 and 7 argue very strongly that Bpa4 has cross-linked into Met35. We have determined not only the residue at which the photoinsertion has occurred but also the precise location of the cross-link within the benzoylphenylalanine and methionine side chains.

Determination of the position of the cross-link between Bpa4 and Met35 results in a high-resolution structural constraint on Aβ molecules within amyloid fibrils. Photoaffinity cross-linking experiments with amyloid fibrils composed of the M35Nle peptide demonstrate that the Bpa4−Met35 cross-link is not an artifact resulting from a preferential affinity of the benzophenone radical for methionine but a result that provides valid structural information on interstrand contact regions between assembled Aβ peptide subunits. This single constraint places the N-terminus of one Aβ molecule and the C-terminus of an adjacent Aβ molecule in close (<3 Å) juxtaposition. Assuming peptide molecules are in register or nearly in register, as found in several studies (*17*, *18*, *21*, *22*, *27*), such a juxtaposition indicates that adjacent peptide molecules are aligned in an antiparallel fashion. Moreover, the cross-link between Bpa4 and Met35 suggests that the aligned strands are shifted two residues out of register, consistent with the alignment seen in the SSNMR studies of the $A\beta_{34-42}$ fragment (*21*). In general, photolabeling experiments are limited to positive results and cannot rule out other structures that could exist but fail to be detected. We utilized MALDI-TOF mass spectrometry, an extremely sensitive analytical method, for detection of cross-linked structures. Therefore, it is likely that the predominant alignment of Aβ molecules within β-sheet fibrils is an antiparallel alignment, placing Met35 and Phe4 from two adjacent β-strands in close proximity. Parallel structures that cannot be ruled out on the basis of our data include parallel alignment with β-strands shifted +31 (or −9) amino acids out of register and a predominantly parallel structure with antiparallel alignment at the edges of unit cells. Furthermore, our data do not address putative intramolecular β-hairpins that are proposed in some structural models of Aβ (*19*, *46*). Experiments with photoreactive Aβ molecules in which the photophore is placed at different positions in the $A\beta_{1-40}$ peptide sequence to produce additional alignment constraints are underway.

Amyloid fibrils are defined by their unique tinctorial properties that result from the common structural organization of the various peptides or proteins of which they are made. The similarity of X-ray fiber diffraction, FTIR, and SSNMR data collected on various types of amyloid fibrils further points to a shared structural motif. It is widely accepted that the amyloidogenic subunits assemble into β-sheets arranged perpendicular to the long axis of the fiber (cross-β structure). The intermolecular alignment of adjacent β-strands has not been determined. Spectroscopic methods have been unable to achieve consensus on the nature of the structural organization. In this work we present a biochemical approach to the problem. The approach was successful in the determination of an intermolecular contact between amino acids on adjacent amyloid molecules within the fibrillar structure. The determination of these intermolecular interactions between amyloidogenic subunits should enhance understanding of how amyloid forms and assist in the design of pharmacological inhibitors for intervention in the pathogenesis of amyloidoses.

ACKNOWLEDGMENT

We thank Dr. George Smulian for the use of his MALDI-TOF instrument, Dr. Jonathan Lee for $A\beta_{1-40}$-NH_2 M35Nle, and Dr. Randal Morris for his assistance with the EM studies.

REFERENCES

1. Maggio, J. E., and Mantyh, P. W. (1996) *Brain Pathol. 6*, 147−162.
2. Iqbal, K. (1991) *Prevalence and neurobiology of Alzheimer's disease*, John Wiley and Sons, New York.
3. Alzheimer, A. (1906) *Neurol. Centr. 23*, 1129−1136.
4. Cummings, B. J., and Cotman, C. W. (1995) *Lancet 346*, 1524−1528.
5. Cummings, B. J., Pike, C. J., Shankle, R., and Cotman, C. W. (1996) *Neurbiol. Aging 17*, 921−933.
6. Cai, X. D., Golde, T. E., and Younkin, S. G. (1993) *Science 259*, 514−516.
7. Citron, M., Oltersdorf, T., Haass, C., McConlogue, L., Hung, A. Y., Seubert, P., Vigo-Pelfrey, C., Lieberburg, I., and Selkoe, D. J. (1992) *Nature 360*, 672−674.
8. Rogaev, E. I., Sherrington, R., Rogaeva, E. A., Levesque, G., Ikeda, M., Liang, Y., Chi, H., Lin, C., Holman, K., Tsuda, T., et al. (1995) *Nature 376*, 775−778.
9. Sherrington, R., Rogaev, E. I., Liang, Y., Rogaeva, E. A., Levesque, G., Ikeda, M., Chi, H., Lin, C., Li, G., Holman, K., et al. (1995) *Nature 375*, 754−760.
10. Games, D., Adams, D., Alessandrini, R., Barbour, R., Berthelette, P., Blackwell, C., Carr, T., Clemens, J., Donaldson, T., Gillespie, F., et al. (1995) *Nature 373*, 523−527.
11. Pike, C. J., Burdick, D., Walencewicz, A. J., Glabe, C. G., and Cotman, C. W. (1993) *J. Neurosci. 13*, 1676−1687.
12. Lorenzo, A., and Yankner, B. A. (1994) *Proc. Natl. Acad. Sci. U.S.A. 91*, 12243−12247.
13. Hartley, D. M., Walsh, D. M., Ye, C. P., Diehl, T., Vasquez, S., Vassilev, P. M., Teplow, D. B., and Selkoe, D. J. (1999) *J. Neurosci. 19*, 8876−8884.
14. Frautschy, S. A., Baird, A., and Cole, G. M. (1991) *Proc. Natl. Acad. Sci. U.S.A. 88*, 8362−8366.
15. Weldon, D. T., Rogers, S. D., Ghilardi, J. R., Finke, M. P., Cleary, J. P., O'Hare, E., Esler, W. P., Maggio, J. E., and Mantyh, P. W. (1998) *J. Neurosci. 18*, 2161−2173.
16. Serpell, L. C., Fraser, P. E., and Sunde, M. (1999) *Methods Enzymol. 309*, 526−536.
17. Kirschner, D. A., Inouye, H., Duffy, L. K., Sinclair, A., Lind, M., and Selkoe, D. J. (1987) *Proc. Natl. Acad. Sci. U.S.A. 84*, 6953−6957.
18. Halverson, K. J., Sucholeiki, I., Ashburn, T. T., and Lansbury, P. T. (1991) *J. Am. Chem. Soc. 113*, 6701−6703.
19. Hilbich, C., Kisters-Woike, B., Reed, J., Masters, C. L., and Beyreuther, K. (1991) *J. Mol. Biol. 218*, 149−163.
20. Krimm, S., and Bandekar, J. (1986) *Adv. Protein Chem. 38*, 181−364.
21. Lansbury, P. T., Jr., Costa, P. R., Griffiths, J. M., Simon, E. J., Auger, M., Halverson, K. J., Kocisko, D. A., Hendsch, Z. S., Ashburn, T. T., Spencer, R. G., et al. (1995) *Nat. Struct. Biol. 2*, 990−998.
22. Benzinger, T. L., Gregory, D. M., Burkoth, T. S., Miller-Auer, H., Lynn, D. G., Botto, R. E., and Meredith, S. C. (1998) *Proc. Natl. Acad. Sci. U.S.A. 95*, 13407−13412.
23. Gregory, D. M., Benzinger, T. L., Burkoth, T. S., Miller-Auer, H., Lynn, D. G., Meredith, S. C., and Botto, R. E. (1998) *Solid State Nucl. Magn. Reson. 13*, 149−166.
24. Benzinger, T. L., Gregory, D. M., Burkoth, T. S., Miller-Auer, H., Lynn, D. G., Botto, R. E., and Meredith, S. C. (2000) *Biochemistry 39*, 3491−3499.
25. Hilbich, C., Kisters-Woike, B., Reed, J., Masters, C. L., and Beyreuther, K. (1992) *J. Mol. Biol. 228*, 460−473.
26. Esler, W. P., Stimson, E. R., Ghilardi, J. R., Lu, Y. A., Felix, A. M., Vinters, H. V., Mantyh, P. W., Lee, J. P., and Maggio, J. E. (1996) *Biochemistry 35*, 13914−13921.
27. Antzutkin, O. N., Balbach, J. J., Leapman, R. D., Rizzo, N. W., Reed, J., and Tycko, R. (2000) *Proc. Natl. Acad. Sci. U.S.A. 97*, 13045−13050.
28. Balbach, J. J., Ishii, Y., Antzutkin, O. N., Leapman, R. D., Rizzo, N. W., Dyda, F., Reed, J., and Tycko, R. (2000) *Biochemistry 39*, 13748−13759.
29. Behar, V., Bisello, A., Bitan, G., Rosenblatt, M., and Chorev, M. (2000) *J. Biol. Chem. 275*, 9−17.
30. Hadac, E. M., Pinon, D. I., Ji, Z., Holicky, E. L., Henne, R. M., Lybrand, T. P., and Miller, L. J. (1998) *J. Biol. Chem. 273*, 12988−12993.
31. Li, Y. M., Marnerakis, M., Stimson, E. R., and Maggio, J. E. (1995) *J. Biol. Chem. 270*, 1213−1220.
32. Zhang, J. H., Stobb, J. W., Hanesworth, J. M., Sardinia, M. F., and Harding, J. W. (1998) *J. Pharmacol. Exp. Ther. 287*, 416−424.
33. Dorman, G., and Prestwich, G. D. (1994) *Biochemistry 33*, 5661−5673.
34. Prestwich, G. D., Dorman, G., Elliott, J. T., Marecak, D. M., and Chaudhary, A. (1997) *Photochem. Photobiol. 65*, 222−234.
35. O'Neil, K. T., and DeGrado, W. F. (1989) *Proteins 6*, 284−293.
36. Maggio, J. E., Stimson, E. R., Ghilardi, J. R., Allen, C. J., Dahl, C. E., Whitcomb, D. C., Vigna, S. R., Vinters, H. V., Labenski, M. E., and Mantyh, P. W. (1992) *Proc. Natl. Acad. Sci. U.S.A. 89*, 5462−5466.
37. Podlisny, M. B., Walsh, D. M., Amarante, P., Ostaszewski, B. L., Stimson, E. R., Maggio, J. E., Teplow, D. B., and Selkoe, D. J. (1998) *Biochemistry 37*, 3602−3611.
38. Walsh, D. M., Lomakin, A., Benedek, G. B., Condron, M. M., and Teplow, D. B. (1997) *J. Biol. Chem. 272*, 22364−22372.
39. Biere, A. L., Ostaszewski, B., Stimson, E. R., Hyman, B. T., Maggio, J. E., and Selkoe, D. J. (1996) *J. Biol. Chem. 271*, 32916−32922.
40. Esler, W. P., Stimson, E. R., Mantyh, P. W., and Maggio, J. E. (1999) *Methods Enzymol. 309*, 350−374.
41. Schagger, H., and von Jagow, G. (1987) *Anal. Biochem. 166*, 368−379.
42. Shevchenko, A., Wilm, M., Vorm, O., and Mann, M. (1996) *Anal. Chem. 68*, 850−858.
43. Kocher, F., Favre, A., Gonnet, F., and Tabet, J. (1998) *J. Mass Spectrom. 33*, 921−935.
44. Jones, M. D., Merewether, L. A., Clogston, C. L., and Lu, H. S. (1994) *Anal. Biochem. 216*, 135−146.
45. Fraser, P. E., Duffy, L. K., O'Malley, M. B., Nguyen, J., Inouye, H., and Kirschner, D. A. (1991) *J. Neurosci. Res. 28*, 474−485.
46. Serpell, L. C. (2000) *Biochim. Biophys. Acta 1502*, 16−30.

BI002852H